

# Interference Management for Future Cellular OFDMA Systems Using Coordinated Multi-Point Transmission

Lars THIELE<sup>†a)</sup>, Volker JUNGNICHEL<sup>†</sup>, and Thomas HAUSTEIN<sup>†</sup>, *Members*

**SUMMARY** Today's cellular systems reach their limits for data rate due to the continuously increasing amount of subscribers using wireless service for business purposes or in leisure time (smartphone effect). Thus, recent research focuses on concepts for interference management for cellular OFDMA systems. This paper addresses various techniques related to this topic, while considering the concepts with lowest complexity and backhaul costs as promising candidates to be applied first. Starting from interference canceling receivers over multi-user MIMO using fixed precoding to multi-cell interference estimation, which improves the precision of link adaptation, we discuss closed-loop cooperative transmit beamforming using multiple base stations grouped into a wireless distributed network (WDN), which is denoted as coordinated multi-point joint transmission in the 3GPP LTE-Advanced standardization. It is obvious, the more sophisticated these techniques are, the higher the demands for feedback and backhaul become. Performance results are provided by employing multi-cell simulations according to recommendations from 3GPP. In addition, feasibility of coordinated multi-point joint transmission is demonstrated in a real-time prototype setup, i.e. in the Berlin LTE-Advance Testbed.

**key words:** WDN, interference management, CoMP, joint transmission

## 1. Introduction

In order to satisfy the continuously increasing demands of emerging wireless services, future mobile cellular networks will operate with full frequency reuse and higher base stations (BSs) density to achieve high spectral efficiencies. However, inter-cell interference becomes soon a limiting factor. Transmission techniques such as hybrid ARQ, adaptive modulation and turbo coding as well as multiple-input multiple-output (MIMO)-orthogonal frequency division multiplex (OFDM) and multiuser scheduling reach a network performance that can hardly be enhanced further from a single-cell point of view.

Recent research investigates concepts for combating the effects of cochannel interference (CCI) in mobile networks by using MIMO techniques [1]. These concepts cover interference canceling receivers, multi-user MIMO (MU-MIMO) (Fig. 1(a)) and finally closed-loop cooperative transmit beamforming using multiple BSs, which is denoted as coordinated multi-point (CoMP) joint transmission (JT) in the 3GPP LTE-Advanced standardization (Fig. 1(b)). The more sophisticated these techniques are, the more feedback is required. Note, for CoMP channel state information at the transmitter (CSIT) is required. This can be achieved

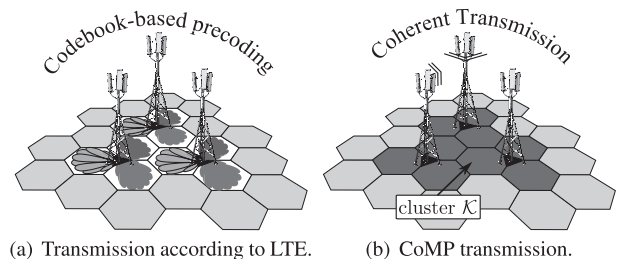


**Fig. 1** From codebook based, decentralized transmission to coherent, joint transmission of collaborative base stations.

by measuring the channel in reverse direction and exploiting reciprocity in time division duplex (TDD) systems. In frequency division duplex (FDD) systems, which is in the focus of this paper, the channel is measured in the downlink direction and channel state information (CSI) is fed back in the uplink.

For the scheduling in one cell, user equipments (UEs) provide feedback on their signal to interference and noise ratios (SINRs) in the form of so-called channel quality indicator (CQI) values for subgroups of subcarriers denoted as physical resource blocks (PRBs). These CQIs correspond to a specific spatial transmission mode, which is indicated by the precoding matrix indicator (PMI). When multiple users are served on the same PRB, the spatial multiplexing (SMUX) transmission mode [2] is generalized from single-user MIMO (SU-MIMO) to MU-MIMO transmission.

As a first extension towards multi-cell processing, adjacent base stations are synchronized and multi-cell demodulation reference signals (DRS) are introduced. They enable interference-aware equalization at the UE and improve the SINR estimation accuracy, leading to a more precise link adaptation at the BS side [3].

The system performance can be further improved, by introducing multi-cell CSI feedback from the UE to the serving BS. Thus, BSs can determine the optimal beamforming weights for the set of users multiplexed on the same PRB in adjacent cells. Early concepts considered a huge centralized wireless distributed network (WDN), where all BS antenna are connected via a fast backhaul link to a central unit (CU) [4]–[7]. Non-linear signal pre-processing, known as dirty paper precoding [8], was shown to achieve the broadcast channel (BC) capacity [9], [10]. By allowing full coordination among the whole network and thus removing the complete interference, the system throughput is lower-bounded by the performance of isolated cells [11].

Manuscript received August 11, 2010.

Manuscript revised August 26, 2010.

<sup>†</sup>The authors are with Fraunhofer Heinrich Hertz Institute, Germany.

a) E-mail: lars.thiele@hhi.fraunhofer.de

DOI: 10.1587/transcom.E93.B.3228

In theory, this yields a block diagonal receive covariance matrix. Of course, this requires additional feedback overhead, since each UE has to convey the full multi-cell MIMO channel coefficients measured at the antenna ports of the serving cell in addition to the CQI. An extension of the block diagonalization concept called multi-user eigenmode transmission (MET) is proposed in [12]. It assumes a linear transmission strategy based on zero-forcing beamforming in combination with Eigenmode feedback from each UE. The Eigenmode concept was shown to reduce the peak-to-average power ratio (PAPR) for linear precoding [13] as well as for non-linear Tomlinson-Harashima precoding (THP) [14]. In general, by limiting each user to report its strongest eigenmodes only, feedback may be reduced.

There are several arguments in favor of limiting the coordination to a cluster of cells. Realistic wave propagation implies that inter-cell interference is spatially limited to the nearest-neighbor cells. Beside the typical urban path loss exponents in the order of 3 to 4, interference is rather localized if 3D radiation characteristics of real-world BS antennas are included [15]. These antennas form a narrow beam with a half-power beam-width of roughly  $6^\circ$  in elevation and  $60^\circ$  in azimuth covering one sector (Kathrein 80010541). Moreover, the beam can be tilted down to limit the effective cell size. Therefore, we assume that a high fraction of the CoMP gains could be realized already with small or medium size clusters of coordinated base stations. This is another way to reduce the overhead. The number of orthogonal pilots for the multi-cell channel estimation, the effort for the feedback over the uplink and the backhaul traffic for the information exchange between the BSs essentially scale with the cluster size. On the other hand, there is always a residual interference floor from non-coordinated cells surrounding the cluster. Thus, the performance depends critically on the cluster size and the interference scenario. We intuitively approach the information-theoretic limit of fully coordinated cells if the cluster size tends to infinity.

At this point, we need to clarify the usage of three different terms: *decentralized*, *centralized* and *distributed*. In case of a *decentralized* system concept, each BS is assumed to have no feedback information, in particular no CSI, from other BS's users. In contrast, the *centralized* system concept assumes full CSIT shared among all BSs in the cluster. And finally, the term *distributed* indicates that a specific system concept can be implemented in a distributed manner, i.e. without a central unit (CU).

The paper is organized as follows. Section 2 introduces the system model which is valid for precoded downlink transmission for a scalable cluster size  $K$ . In Sect. 3, the precoding matrices are constructed according to the codebooks defined for long term evolution (LTE) systems and potential key drivers for decentralized interference management are discussed and evaluated in a system level simulator. The simulation results from Sect. 3 are considered as a reference case for the following paragraphs. Section 4 describes a concept for distributed CoMP JT, where Sects. 4.2 and 5 evaluate its performance by using multi-cell simulations and

demonstrate its feasibility in a prototype field trail system, i.e. the Berlin LTE-Advanced Testbed. The paper is concluded in Sect. 6.

## 2. System Model

We consider a cellular OFDM downlink where a central site is surrounded by multiple tiers of sites. We assume each site to be partitioned into three  $120^\circ$  sectors, i.e. a set  $\mathcal{L}$  consisting of  $L = |\mathcal{L}|$  sectors in total. Each sector constitutes a cell, and frequency resources are fully reused in all  $L$  cells. Each cell is controlled by a BS. If CoMP JT is allowed, the data to each user is simultaneously transmitted from multiple BSs. In order to limit the overhead related to joint processing techniques, BSs are grouped into subsets of cells denoted as *clusters*, refer to Fig. 1(b).  $\mathcal{K}$  represents the set of cells included in a given cluster and  $K = |\mathcal{K}|$  denotes its maximum dimension. Joint processing is only allowed between BSs belonging to the same cluster, whereas BSs belonging to different clusters are not coordinated and thus produce residual inter-cluster interference. Further, we assume disjoint clusters, i.e. a given BS cannot belong to more than one cluster operated at the same time/frequency resource. For OFDM systems, the overlap of multiple clusters can be achieved conveniently in the frequency domain. Hence, in the  $i$ th cluster, there are  $K$  BSs, each one equipped with  $N_T$  transmit antennas, and a set of  $\mathcal{M}_{all}$  multi-antenna users, each equipped with  $N_R$  receive antennas. This cluster-user constellation is valid for a particular resource and may vary over time and frequency. In addition, we assume a scheduling instance, which selects a specific set of active users  $\mathcal{M} \subset \mathcal{M}_{all}$  within the cluster, with  $M = |\mathcal{M}|$  being the number of active users. In particular, the subset  $\mathcal{M}_k$  combines those users experiencing highest channel gain to the  $k$ th BS. The downlink MIMO-OFDM transmission system is described on a per sub-carrier basis

$$\mathbf{y} = \mathbf{H}_i \mathbf{C}_i \sqrt{\mathbf{P}_i} \mathbf{x} + \mathbf{n}, \quad (1)$$

where  $\mathbf{H}_i$  is the  $MN_R \times KN_T$  channel matrix,  $\mathbf{C}_i$  is the  $KN_T \times KN_T$  precoding matrix and  $\mathbf{P}_i$  is the power allocation matrix of dimension  $KN_T \times KN_T$ ;  $\mathbf{x}$  denotes the  $KN_T \times 1$  vector of transmit symbols;  $\mathbf{y}$  and  $\mathbf{n}$  denote the  $MN_R \times 1$  vectors of the received signals and of the additive white Gaussian noise (AWGN) samples, respectively, with covariance  $E[\mathbf{nn}^H] = \sigma_n^2 \mathbf{I}$ .  $E[\cdot]$  is the expectation operator.

Depending on the deployment of the BSs and the actual position of the UE, the user will receive interfering signals sent to other users in parallel to its desired signal. Appropriate antenna downtilting at the BS side helps to adjust the effective cell size to a desired value. This keeps cochannel interference (CCI) localized, i.e. the interference mainly comes from adjacent cells with respect to user's actual position [15]. The users inside the cluster are served by signals jointly emitted from  $KN_T$  transmit antennas, where  $K \cdot N_T \geq M \cdot N_R$ . Assuming a linear precoding strategy, there can be  $KN_T$  data streams coherently transmitted by

using specific precoding vectors (beams). In particular, the  $KN_T \times KN_T$  precoding matrix  $\mathbf{C}_i = [\mathbf{b}_{i,1} \cdots \mathbf{b}_{i,M}]$  contains the precoders  $\mathbf{b}_{i,m}$  designed for each of the users in  $\mathcal{M}$ . Correspondingly, the beams constitute the columns in the precoding matrix  $\mathbf{C}_i$ .

For further analysis, we assume the  $i$ -th cluster is surrounded by  $L - K$  BSs evoking non-coordinated CCI. Thus, the received downlink signal  $\mathbf{y}_m$  at the UE  $m$  in the cellular environment is given by

$$\mathbf{y}_m = \underbrace{\mathbf{H}_{i,m} \mathbf{b}_{i,m}}_{\bar{\mathbf{h}}_m} \sqrt{p_{i,m}} x_{i,m} + \underbrace{\sum_{j=1, j \neq m}^M \mathbf{H}_{i,m} \mathbf{b}_{i,j} \sqrt{p_{i,j}} x_{i,j}}_{\zeta_m} + \underbrace{\sum_{\substack{l \in \mathcal{L} \setminus \mathcal{K} \\ \forall j=1}}^{N_T} \mathbf{H}_{l,m} \mathbf{b}_{l,j} \sqrt{p_{l,j}} x_{l,j}}_{\mathbf{z}_m} + \mathbf{n} \quad (2)$$

The desired data stream  $x_{i,m}$  transmitted to the  $m$ th user from the  $i$ th cluster is distorted by the intra-cluster and inter-cluster interference plus noise aggregated in  $\zeta_m$  and  $\mathbf{z}_m$ , respectively.  $\mathbf{H}_{i,m}$  spans the  $N_R \times KN_T$  channel matrix for user  $m$  formed by the  $i$ th cluster and  $p_{i,m}$  is its power allocation. Thus,  $\zeta_m$  denotes the interference generated within the cluster. The achievable SINR is estimated at each UE, according to

$$\text{SINR}_m = \frac{|\mathbf{w}_m^H \mathbf{H}_{i,m} \mathbf{b}_{i,m}|^2 p_{i,m}}{\sum_{j=1, j \neq m}^M |\mathbf{w}_m^H \mathbf{H}_{i,m} \mathbf{b}_{i,j}|^2 p_{i,j} + \mathbf{w}_m^H [\mathbf{z}_m \mathbf{z}_m^H] \mathbf{w}_m}, \quad (3)$$

with  $\mathbf{w}_m$  being the combining weights at the receiver, e.g. maximum ratio combining (MRC) or optimum combining (OC) [16].

### 3. Decentralized Interference Management

#### 3.1 Concept

At first, we investigate a practical solution for decentralized interference management, where BSs are not required to exchange any user payload data. Thus, we consider to use fixed beams for transmission as depicted in Fig. 1(a). Assume that all BSs provide  $\Omega$  fixed unitary beam sets  $\mathbf{C}_\omega$ ,  $\omega \in \{1, \dots, \Omega\}$ . For the case of  $N_T = 2$  and  $\Omega = 2$  the beam sets are based on the pairs of orthogonal columns in the first two rows of the 4-DFT-matrix according to [17]

$$\mathbf{C}_1 = \frac{1}{\sqrt{2}} \begin{bmatrix} 1 & 1 \\ i & -i \end{bmatrix} \quad \mathbf{C}_2 = \frac{1}{\sqrt{2}} \begin{bmatrix} 1 & 1 \\ 1 & -1 \end{bmatrix} \quad (4)$$

In general, each beam set contains  $N_T$  fixed precoding vectors (beams)  $\mathbf{b}_{\omega,u}$  with  $u \in \{1, \dots, N_T\}$ . Terminals are assumed to report their preferred precoding indices, i.e. PMI, in combination with corresponding post-equalization SINRs

via a low-rate feedback channel, refer to Fig. 3(a). Therefore, each UE assumes its preferred MIMO transmission mode, i.e. single-stream or multi-stream<sup>†</sup> transmission. It is quite obvious, that the system performance depends on the granularity of the feedback in all dimensions, i.e. the number of combined PRBs, the granularity of the SINR quantization which enables more or less precise adaptation to the channel using a set of modulation and coding scheme (MCS) and the granularity of the codebook used for the spatial precoding over multiple transmit antennas<sup>††</sup>.

For OC, which also known as as interference rejection combining (IRC), we use the interference-aware minimum mean square error (MMSE) receiver:

$$\mathbf{w}_u^{\text{MMSE}} = p_u \mathbf{R}_{yy}^{-1} \bar{\mathbf{h}}_{i,u} \quad (5)$$

The required channel plus interference knowledge may be obtained by multi-cell channel estimation based on block-orthogonal pilot symbols, denoted as DRS. Our proposal is to multiply subsequently transmitted pilots symbols by a cell-specific sequence  $c_{i,u}(n)$ . The maximum number of transmitted pilot symbols  $N$  defines the number of orthogonal channel groups, which may be resolved by correlation with the given code. In order to reduce the interference within one sequence group, we can maximize the distance between cells using the same sequence [18].

$$\hat{\mathbf{h}}_{i,u} = \frac{1}{N} \sum_{n=0}^{N-1} c_{i,u}^*(n) \mathbf{y}^m(n) \quad (6)$$

Note, we have to ensure that reference signals from multiple BSs are transmitted coherently and are received within the given cyclic prefix (CP) at the UE. Thus, downlink transmission has to be synchronized [19]. The covariance matrix of the multi-cell MIMO channel is given by

$$\mathbf{R}_{yy} = \sum_{\forall l,j} \hat{\mathbf{h}}_{l,j} \hat{\mathbf{h}}_{l,j}^H \quad (7)$$

According to the feedback provided by each UE, i.e. CQI and PMI, each BS can independently adapt to a desired entry in the codebook in order to serve their users in an optimized way. The selected scheduling policy should operate in a decentralized manner, which helps to reduce deployment complexity and delays in the system. Furthermore, frequency-selective multi-user scheduling can provide significant gains by exploiting both, frequency and multi-user selection diversity. A favorable solution, which tends to assign each user his best resources, is the score-based scheduling policy described in [20]. Clearly, the process is of heuristic nature, and hence the global scheduling target of assigning each user an equal amount of resources is achieved on average only or if the number of available resources tends to infinity. In [21] it was extended to cover

<sup>†</sup>Where multiple streams can be transmitted to a single user, i.e. SU-MIMO, or to multiple user, i.e. MU-MIMO.

<sup>††</sup>In general, the gap to Shannon information rates is the smaller the coarser the granularity of any such quantization is.

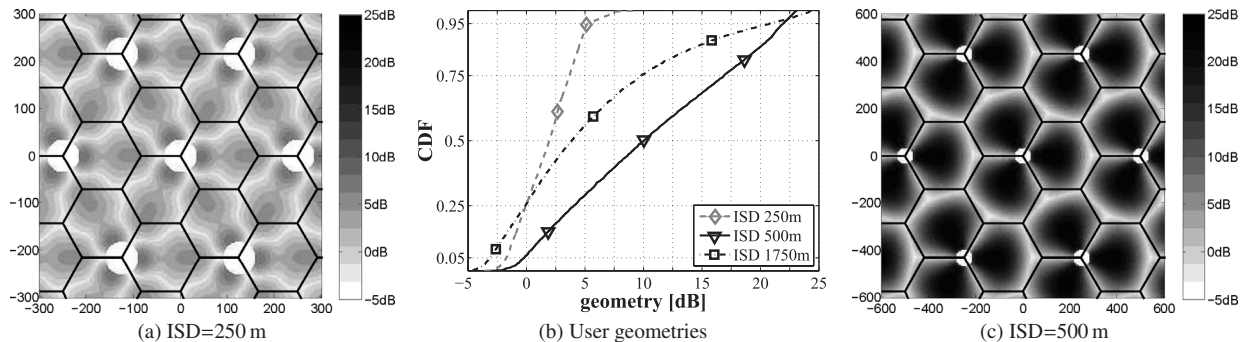


**Fig. 2** Downtilt angle is set to  $10^\circ$  at 32 m BS antenna height. The main lobe hits the ground at  $\frac{1}{3}$ ISD for ISD = 500 m, resulting in the best user geometry. The inter-site distance (ISD) is varied from 250 m, over 500 m up to 1750 m. White dots indicate the range where the path loss model is not valid and thus UEs cannot be placed.

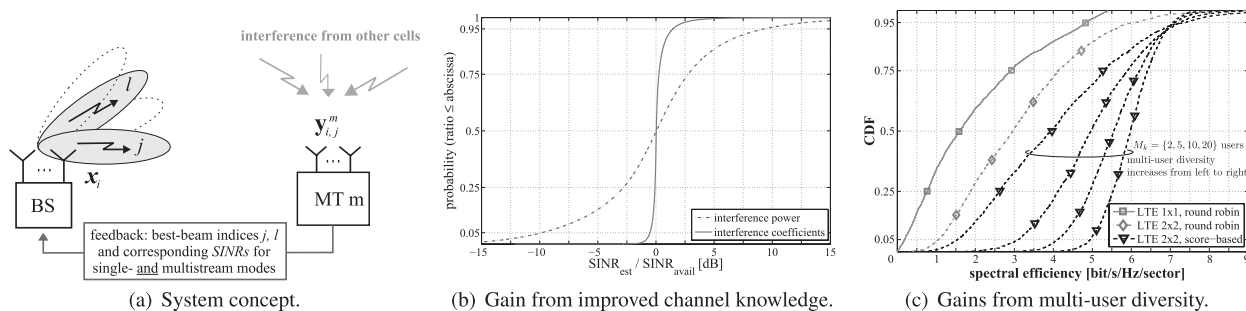


**Fig. 3** (a) Quantized SINR values, i.e. CQIs, are provided by the terminal for possible transmission modes using a narrow band feedback channel. In addition the best beam indices, i.e. PMIs, are reported to the base station. (b) Error in the SINR estimation process at the UE side, under the assumption of knowledge on interference power only or estimation of channel coefficient to the most prominent interfering BS sites. (c) Diversity gains from multiple users and frequency selective scheduling.

MIMO mode switching. In order to keep the dominant CCI predictable, we have to assume, that BSs in a cluster know a change in downlink power allocation. This might be the case, if BSs change the MIMO transmission mode from multi-stream to single-stream transmission or vice versa. In the case of coordinated scheduling/beamforming (CS/CB) [22], [23], multiple BSs can be grouped into a cluster  $\mathcal{K}$ , where all  $K$  BSs can jointly optimize the selection of entries from the codebook. Note, in general this leads to a constrained selection of frequency and spatial resources, where a limited set of resources can be reused at all BSs in  $\mathcal{K}$ .

### 3.2 Multi-Cell Simulation Results

The concept of decentralized interference management without CS/CB is evaluated in a triple-sector hexagonal cellular network with  $L = 57$  BS sectors in total. All sectors operate at the same frequency band, i.e. the frequency reuse factor equals one. We employ the wrap-around technique, which ensures that the interference scenario is complete and follows independent, identical distributed (i.i.d.) statistics for all users. The different channel matrices are generated by employing the widely used spatial channel model extended (SCME) [24] with urban macro scenario parameters [25] and 3D BS antenna characteristics. Figure 2

depicts the achievable user geometries as a function of the ISD while keeping the downtilt angle fixed to  $10^\circ$ . With decreasing ISDs, the cellular system becomes more and more interference limited. On the other hand, with larger ISD the system becomes noise-limited. Throughout all simulation results in this paper, we set the electrical downtilt to  $10^\circ$  and the ISD to 500 m. The resulting main lobe range of  $\frac{1}{3}$ ISD is a favorable property, since it yields a relatively high cell isolation and thus leads to best performances for the case of non cooperating BSs.

Figure 3(b) depicts the estimation error for different degree of channel plus interference knowledge, which is used as inputs for the equalization process from (5) and (3). In particular, it shows the ratio of the estimated versus the theoretical available SINR when using both, simple interference power estimation or received interference covariance estimation based on multi-cell DRS, with  $N = 12$  in a quasi-static channel. Thus, by employing OC with adequate channel knowledge, we can significantly improve the estimation accuracy of SINRs at the receiver side and thus improve the precision of the link adaptation process.

Figure 3(c) depicts the cumulative distribution function (CDF) curves for the system spectral efficiency using adaptive modulation and coding per PRB, while assuming the MCS levels as defined for LTE. Further, we assume an error-

free link-adaptation, i.e. a perfect SINR estimation. For reference purpose, we include results for interference-limited single-input single-output (SISO) as well as a MIMO  $2 \times 2$  transmission. In the case of the SISO setup, the system utilizes only a single spatial dimension. The system with  $N_T = 2$  transmit antennas can offer an additional spatial layer and thus can serve  $M = 2$  different users instantaneously on the same PRB. Accordingly, the spectral efficiency is increased by  $\approx 90\%$  if the spatial layer assignment is carried out in a round-robin manner. The system performance can be further improved if the layer assignment is done while taking the CQI feedback into account. Hence, the CQI-aware score-based solution outperforms both other reference cases with a relative throughput gain of  $\Delta_{K=1} = 1.3$  and  $\Delta_{K=1} = 2.5$  compared to round-robin and SISO case, respectively<sup>†</sup>. For the case of the score-based resource assignment, the spectral efficiency may be further improved by  $\Delta_{K=1, M=5} = 3.1$ ,  $\Delta_{K=1, M=10} = 3.5$  and  $\Delta_{K=1, M=20} = 3.8$  with respect to the SISO setup, where the additional index  $M$  denotes the total number of active users in  $\mathcal{M}$ . For further details on the performance evaluation including channel estimation errors refer to [3], the feasibility of the concept in a real-time prototype is described in [26].

#### 4. Distributed Coordinated Multi-Point Transmission

##### 4.1 Concept for CoMP Joint Transmission (JT)

In modern mobile networks, there is a general tendency of using distributed signal processing. The adaptation to the time variation of the wireless channel can be much faster if it is performed directly in the serving BS. For downlink CoMP, we reduce the overall delay in the closed transmitter adaptation loop if the waveforms are generated at the serving BS. Concepts for a distributed implementation of CoMP, where the serving BS cooperates with a small subset of BSs, Fig. 1(b), in its direct vicinity are reported in [27]–[32]<sup>††</sup>. Recently, we have reported on a first real-time implementation [33], [34] of downlink CoMP demonstrating its feasibility. Terminals are assumed to estimate the multi-cell CSI in the downlink using CSI reference signals (CRS), refer to Fig. 4(b). Subsequently, UEs deliver CSI feedback in combination with CQI values to their serving BS. Next, BSs in the cluster exchange the CSI as well as scheduled user data over a low-latency signaling network denoted as X2 interface (X2 interface) [35]. Precoding weights for the joint beam-forming are determined at each BS. The relevant set of weights is applied to the data signals and in this way, the transmitted waveforms are obtained locally. Similar to the centralized approach, the desired signals sum up constructively while the mutual interference inside the cluster is canceled. We emphasize that under the assumption of low Doppler shift, i.e. for low mobility or even static users, the backhaul bandwidth required for sharing the user data between cooperating BSs is much higher than the one required for updating the channel estimates within the clus-

ter. Let us assume an average throughput per cell denoted as *rate*, hence, each BS has to receive the scheduled user data for its own UEs according to that data rate. Further, we consider that hybrid automatic repeat request (HARQ) processes for each user in the active set of users  $\mathcal{M}_k$  are running decentralized at each BS  $k$ . Thus, each BS has to perform the channel coding with a given *code\_rate*<sup>†††</sup> according to the CQI feedback provided by the users in  $\mathcal{M}_k$ . According to (8), all remaining BSs  $K - 1$  in the cluster  $\mathcal{K}$  convey their coded user data over the backhaul to the  $k$ -th BS<sup>††††</sup>. Thus, the backhaul overhead scales linear with the number of BSs exchanging their scheduled data in the cluster.

$$\text{traffic} = \text{rate} \left( 1 + \frac{K - 1}{\text{code\_rate}} \right) \quad (8)$$

According to Fig. 4(b), the CoMP JT process is split into three phases:

##### 1. Phase I: Channel Feedback.

Each user performs a cluster-wise channel estimation using CRS. Each user equipment (UE) generates multiple-input single-output (MISO)-CSI [12], [32], [36] according to

$$\mathbf{h}_{i,m} = \mathbf{v}_m^H \mathbf{H}_{i,m}, \quad (9)$$

where the Euclidean norm equals  $\|\mathbf{v}_m\|_2 = 1$ . Besides,  $\mathbf{v}_m$  is always used to denote the linear combining scheme to generate CSI MISO feedback. For our results obtained in Sect. 4.2, we assume an eigenmode based feedback scheme known as MET, which was initially proposed for MU-MIMO transmissions [12] and was later extended to cover the CoMP case [32]. In essence, each user is assumed to multiply its channel matrix  $\mathbf{H}_{i,m} = \mathbf{U}_{i,m} \boldsymbol{\Sigma}_{i,m} \mathbf{V}_{i,m}^H$  by the Hermitian of the left dominant eigenvector (10), i.e. the column vector  $\mathbf{u}_{i,m}$  included in  $\mathbf{U}_{i,m}$  which corresponds to the strongest Eigenvalue in  $\boldsymbol{\Sigma}_{i,m}$ , i.e.  $\mathbf{v}_m = \mathbf{u}_{i,m}$ .

$$\mathbf{h}_{i,m} = \mathbf{u}_{i,m}^H \mathbf{H}_{i,m} = \mathbf{u}_{i,m}^H \mathbf{U}_{i,m} \boldsymbol{\Sigma}_{i,m} \mathbf{V}_{i,m}^H = \lambda_{i,m} \mathbf{v}_{i,m}^H \quad (10)$$

Note, for the trials in Sect. 5 we employ a simple receive antenna selection.

The channel information is fed back in conjunction with the expected post-equalization SINR

<sup>†</sup>Where the index  $K = 1$  indicates, that each sector operates independently, i.e. cluster size is equal to 1.

<sup>††</sup>Note, the length of the CP limits the tolerable backhaul latency in the centralized approach. For distributed downlink CoMP, latency is more related to the ongoing aging process of the CSI while it is exchanged over the backhaul. A few ms may be tolerated for slowly moving UE. Hence, capacity and latency requirements for the backhaul are significantly relaxed compared to the centralized approach.

<sup>†††</sup>For the results in Sect. 4.2 we set this rate to 1/2.

<sup>††††</sup>Assuming a virtual local area network (VLAN) topology, data packets can be directed to multiple recipients.

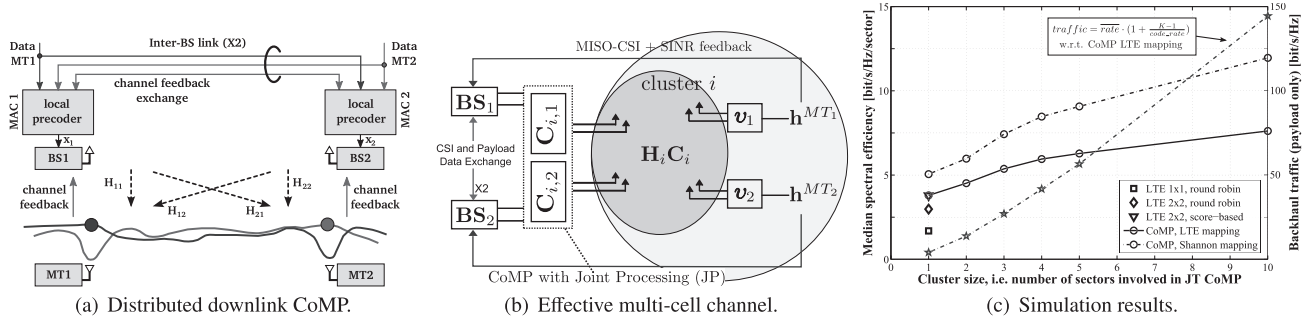


**Fig. 4** (a) and (b) Distributed downlink CoMP: True and effective multi-cell channel. The pre-coder  $\mathbf{C}_i = [(\mathbf{C}_{i,1})^T (\mathbf{C}_{i,2})^T]^T$  for coherent joint transmission can be calculated distributively, while each BS uses the rows corresponding to its antennas. (c) Performance results as a function of the cluster size  $K$ . Channel Feedback is assumed according to the MET concept (10).

$$\text{SINR}_m^{(j)} = \frac{|\mathbf{h}_{i,m} \widehat{\mathbf{b}}_{i,m}|^2 \widehat{p}_{i,m}}{\mathbf{v}_m^H [\mathbf{z}_m \mathbf{z}_m^H] \mathbf{v}_m}. \quad (11)$$

Therefore, each user assumes a power allocation  $\widehat{p}_{i,m}$  as well as a precoder according to  $\widehat{\mathbf{b}}_{i,m} = [\mathbf{h}_{i,m}]^H / \|\mathbf{h}_{i,m}\|_2$  and no intra-cluster interference, since this interference will be removed by the joint precoder. In particular, the achievable SINR (11) together with the CSI (9) is then conveyed to the serving BS.

### 2. Phase II: Distributed precoder calculation.

A scheduling instance in the cluster combines a total number of  $KN_T = MN_T$  MISO channels to a compound MIMO channel matrix<sup>†</sup>. In the following, each BS is responsible for a specific sub-band of the overall bandwidth where CoMP JT is employed. Therefore, BSs exchange their user payload data as well as the collected CSI and combine the channel feedback  $\mathbf{h}_{i,MT_m}$  to a compound virtual MIMO channel matrix of size  $M \times KN_T$  according to (12).

$$\mathbf{H}_{\text{virtual}} = [(\mathbf{h}_{i,MT_1})^T (\mathbf{h}_{i,MT_2})^T \dots (\mathbf{h}_{i,MT_M})^T]^T \quad (12)$$

Subsequently, each BS determines the linear precoder for their specified sub-bands but for all  $KN_T$  antennas of the cluster according to (13).

$$\mathbf{C}_i = \mathbf{H}_{\text{virtual}}^H (\mathbf{H}_{\text{virtual}} \mathbf{H}_{\text{virtual}}^H)^{-1}. \quad (13)$$

Finally, all BSs in the  $i$ -th cluster perform the coherently precoded downlink transmission, where each BS is using the weights corresponding to its own transmit antennas (Tx antennas). In order to meet the per antenna power constraint (PAPC), we use a simplified expression for matrix  $\sqrt{\mathbf{P}_i}$  from [37], where the transmit power per antenna is chosen according to the row element in  $\mathbf{C}_i$  with highest norm. Note, this power allocation typically results in only one BS antenna transmitting with maximum power, and hence, the remaining  $KN_T - 1$  antennas transmit with less than  $P_{\max}/N_T$ .

### 3. Phase III: “Intra-cluster-interference-free” data reception at the terminal side.

In this step, each UE performs its own preferred spatial equalization strategy  $\mathbf{g}_m$ . Therefore, each user may

select the same weights as used in *Phase I* or may perform the equalization using the optimal linear receive combining weights from (5). The post-equalization SINR is determined by (3) and is used as inputs for the link adaptation.

## 4.2 Multi-Cell Simulation Results

The combined receiver-transmitter concepts described above are evaluated in the same multi-cell simulation framework as used in Sect. 3.2. In particular, we determine the system performance by assuming a dynamic and user driven clustering method. However, the system does not utilize any additional gains from multi-user scheduling, i.e. active set of users is selected according to the following metric: A set  $\mathcal{M} = \mathcal{M}_{\text{all}}$  of active multi-antenna terminals is uniformly distributed in the  $i$ -th cluster of the cellular environment. The user selection for each cell is done by a round-robin scheduling policy, yielding a set of users  $\mathcal{M}_k$  of size  $|\mathcal{M}_k| = N_T$ . Note, the users in  $\mathcal{M}_k$  experience highest channel gain to the  $k$ -th BS, i.e. all users are connected to a master BS. In addition, all user sets  $\mathcal{M}_k$  are disjoint for different BSs  $k \in K$ . Further, we emulate a cluster selection which is user-centric and dynamic over frequency: the  $K$  strongest channel gains of the users in  $\mathcal{M}_k$  are the ones of the  $K$  BSs within the cluster. Results are provided for different cluster sizes of  $K \in \{1, 2, 3, 4, 5, 10\}$ . All results in Fig. 4(c) are based on an equal per beam power constraint with a PAPC [37], which is aligned with the assumptions made in LTE.

### 4.2.1 Performance of Reference Cases

For reference purpose, we include the performance results for interference-limited SISO as well as a MIMO  $2 \times 2$  transmission from Sect. 3.2. For  $N_T = 2$ , two active fixed beams are sent to  $M = 2$  different users in a round-robin manner or taking CQI feedback into account.

<sup>†</sup>With a proper user selection, the mandatory full rank condition of the compound channel matrix can be frequently met in the multi-point-to-multi-point channel with independent links [37].

#### 4.2.2 Gain from CSI Feedback and CoMP Transmission

CSI-aware precoding within a given cluster reduces the interference experienced at each UE. Therefore, we use the well-known multi-user eigenmode transmission concept (10). In case of CSI feedback and zero-forcing (ZF) beamforming at a single BS, i.e.  $K = 1$ , with subsequent OC provides a system gain of  $\Delta_{K=1} = 2.5$  and  $\Delta_{K=1} = 1.0$  compared to SISO and score-based beam assignment, respectively. Note, there is no additional gain from CSI based ZF beamforming and a cluster size of  $K = 1$ . This mainly caused by the two facts: First, we assume a simplified PAPC, which leads to a suboptimal power allocation where only one antenna transmits with full power and all others are scaled accordingly [37]. In contrast, in the case of fixed precoding from Sect. 3 all BS antennas transmit with full power. Second, within the score-based spatial layer assignment (reference case), multi-user diversity is used to assign both users to these fixed beams. In the case of ZF beamforming, both users are directly served on orthogonal beams. In both cases the inter-cell interference is not affected.

In the next step, we increase the cluster size for the CoMP system and the gain from MET attributes to  $\Delta_{K=2} = 2.7$ ,  $\Delta_{K=3} = 3.2$ ,  $\Delta_{K=4} = 3.6$ ,  $\Delta_{K=5} = 3.8$  and  $\Delta_{K=10} = 4.6$  w.r.t SISO case. Note, the gap between Shannon information rates and a practical link adaptation according to LTE attributes to 4.3 bit/s/Hz/sector for  $K = 10$ . Concluding, we observe that the median sector spectral efficiencies are increased by 220%, 280% and 360% for coordinating 3, 5 and 10 cells, respectively. However backhaul requirements per feeder link increase as well, i.e. by 5, 9 and 19 bits per bit-on-air-interface assuming a fixed code rate of 1/2, for the coordination of 3, 5 and 10 cells, respectively. Altogether, significant gains from coordination have already been realized by using small clusters, despite the residual interference from non-coordinated clusters.

For  $K = 10$  the estimated median traffic for user (payload) data exchange per backhaul link will exceed a value of 120 bit/s/Hz. This is only a rough estimate according to (8), where  $\overline{rate}$  is the median sector data rate in bit/s/Hz for CoMP transmission using the MCS from LTE. The backhaul traffic consists of the transmitted data over the air interface and the required user data exchange from  $K - 1$  other BSs. Since, BSs have to coherently transmit the same data, i.e. using the same MCS, we consider the BSs to exchange their coded user payload data and independent mapping to identical QAM symbols. For sake of simplicity, we assume here a code rate of 1/2<sup>†</sup>.

### 5. Field Trials in Berlin LTE-Advanced Testbed

In this section we describe our initial real-time implementation and testing of distributed CoMP JT in the downlink of an LTE-Advanced trial network. Enabling features such as distributed synchronization [19], cell- and user-specific pilots and a fast backbone network in which users are served

with data, terminals feed back multi-cell CSI and base stations exchange scheduled data have been implemented and tested in real-time on top of an existing LTE trial system, i.e. in the Berlin LTE-Advanced Testbed. We have implemented the scheme shown in Fig. 4(a) with 2 BSs, 2 UEs having 2 antennas each in FDD mode using 20 MHz bandwidth in the down-link and 10 MHz bandwidth for each UE in the uplink at 2.68 and 2.52 GHz, respectively. For more implementation details, please refer to [33], [34]. Interference-limited transmission experiments have then been conducted using three multi-cell transmission modes. As a lower bound, we use no coordination between the cells but apply per-antenna rate control with interference-aware equalization at the terminal. Second, by using distributed downlink CoMP, the mutual interference between the cells is canceled. Third, we study isolated cells as an upper bound where the interference from other cells is switched off. Trials over the air are described here for indoor and outdoor-to-indoor scenarios covering both intra- and inter-site CoMP. For an outdoor-to-outdoor scenario refer to [34]. We describe impressive observations regarding the reduced outage at the cell edge and demonstrate the huge overall performance improvements when using CoMP JT instead of interference-limited transmission. Clearly these gains are obtained only in the absence of interference from non-coordinated cells. The performance in presence of residual CCI is investigated in Sect. 4.2. Nonetheless, the following experiments demonstrate that the implementation challenges of downlink CoMP can be overcome and that similarly high gains as predicted by the theory can be realized in practice.

#### 5.1 Setup and Scenarios

Scenarios comprise indoor and outdoor-to-indoor configurations, refer to Fig. 5(a). Indoors, both BSs are located in the same lab. In the outdoor-to-indoor scenarios, we transmit from two BS sites and select two sectors either at the same site or at two different sites in order to realize intra- and inter-site cooperation, respectively. Sites are located on the Deutsche Telekom Laboratories (TLabs) building at Ernst-Reuter-Platz (84 m antenna height) and on the Technical University of Berlin (TUB) main building, Straße des 17. Juni (43 m, see Fig. 5(a)). The estimated height of buildings in the area is in between 25 and 35 m. For more insights, refer to [26]. Sites are interconnected by optical fibers deployed in the campus with a length of 4.5 km. The X2 interface signaling over the fiber is based on 1 Gbit/s Ethernet.

For indoor and outdoor-to-indoor scenarios, both UEs are located on the 11th floor at the Fraunhofer Heinrich Hertz Institute (HHI). We placed both UEs at the south front of the building with the windows facing towards both base stations either in the same lab or in two different labs which

<sup>†</sup>Here we do not consider additional overhead due to CSI exchange, which would be only a small part of the overall traffic requirement [38].

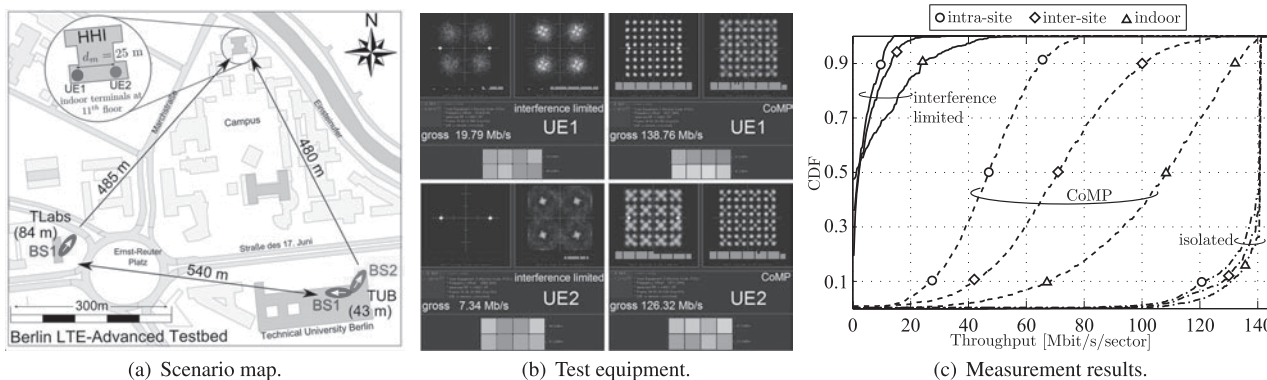


**Fig. 5** (a) Scenario for field trials. (b) For a specific sample of the QAM constellations, measured data rate and received power (red represents a low and green represents a high power level) at both UEs in an interference limited or CoMP scenario. (c) Measurement results for an indoor, an intra-site and an inter-site deployment. Measured throughput for interference-limited transmission (dashed), coordinated multi-point (solid) and isolated cells (dash-dot).

are 25 m separated. UE<sub>2</sub> is at a fixed location. In order to capture the local fading statistics, UE<sub>1</sub> moves at low speed with approximately 3 cm/s. In our implementation, UE<sub>1</sub> is always assigned to BS1 and UE<sub>2</sub> to BS2, i.e. handover is not performed. For performance evaluation, we consider the overall statistics from UEs placed in the same lab and different labs.

### 5.2 Measurement Results

Indoor and outdoor-to-indoor results are plotted in Fig. 5(c). For the current setup, we have a single user assigned to BS1 and a single user assigned to BS2. If we place both UEs at the cell border between BS1 and BS2, both interference scenarios are very similar and thus, similar throughput statistics are obtained. In Fig. 5(c) we show the throughput only for UE<sub>1</sub>. First, as a lower bound, we realize interference-limited transmission using an identity matrix as an independent precoder for BS1 and BS2, in combination with OC at the receiver side. In this case, we have single UE assigned to each BS. Due to limited hardware, the trial system cannot utilize multiuser diversity gains in the frequency selective scheduling, as discussed in Sect. 3 which implies higher outage probability. Next, we have used CoMP JT transmission from both sites with a fixed number of four streams on the air. Finally, as an upper bound, we consider the case of isolated cells where the interference from the other cell is present, i.e. either BS1 or BS2 is switched of.

In the indoor scenario, both BSs are received with the same average power in a rich scattering environment. The average SINR is around 0 dB in both cells simultaneously. Due to multiple reflections in the room, however, both the signal and the interference experience fading. Statistically independent fading of both signals creates a crucial throughput situation for a UE: When moving the UE by a few cm only, we can realize situations where either the signal channel is strong while the interference is in a fade, and correspondingly the serving BS assigns data transmission in

a certain part of the whole frequency band, as well as the reverse situation where the interference channel is strong while the signal is in a fade so that no more data are usually transmitted. Note, the BS assignment is always kept fixed, i.e. BS1 serves UE<sub>1</sub> and BS2 serves UE<sub>2</sub>. As a consequence, the terminal suffers from bad SINR conditions and thus the outage probability amounts to 50%. Thus, the data traffic is not continuous but frequently interrupted when moving through the lab and the user experience may be quite poor.

If CoMP is enabled in such a bad interference scenario, we observe significant improvements for the data throughput. Despite the critical interference situation and although the data rate still varies, CoMP removes outage completely. Using CoMP in such indoor deployments, provides 18 times higher data rates for UEs with respect to the interference limited setup. Note, we realize approximately 78% of the rate achievable in the isolated cell setup.

Next consider the intra-site scenarios. It is typical in the distributed multi-cell network that path losses are not equal for different pairs of BSs and UEs. Nonetheless, the basic observations remain similar. In the interference-limited case, again there is significant outage. Using CoMP, in contrast, both UEs can realize 30% of the peak data rate on average. Note, in this scenario both UEs are placed in the same building, while both serving BSs are situated at the same site, i.e. same antenna pole. In this case, signals transmitted from both sectors show high correlation [39].

The performance in the inter-site scenarios is superior compared to the intra-site scenarios, despite distributed synchronization of both base stations. Studies of the underlying channel correlations suggest that the higher data rates observed with CoMP in the inter-site scenarios may also be attributed to the lower transmit antenna correlation [39] if terminals are not sufficiently separated in the deployment. However, in [34] we demonstrate, the difference between intra-site and inter-site CoMP transmission is rather small when UEs are placed at different buildings or streets in the scenario, i.e. each UE is dominantly served from a different

BS sector.

## 6. Conclusion

In this paper, we investigated promising techniques for interference management in future cellular OFDMA systems. The concepts range from independent scheduling in each cell, over downlink interference estimation to coordinated multi-point joint transmission, where multiple BSs are grouped into a wireless distributed network (WDN). In particular, by using multi-cell simulations, we demonstrated significant gains from a first extension towards multi-cell processing, where adjacent base stations are synchronized and multi-cell demodulation reference signals are introduced. Both enables interference-aware equalization at the UE and improves the SINR estimation yielding a more precise link adaptation at the BS. Finally, we introduced a centralized scheme for coordinated multi-point transmission in the downlink of next generation mobile networks. Therefore, we consider coordinated multi-point joint transmission inside a limited cluster of cells forming an intra-cluster interference free island. This island is surrounded by multiple non-coordinated cells. Again, by employing multi-cell simulations, we evaluated the system performance and demonstrated significant gains from coordination, which can be realized by using small clusters, i.e. gains in the order of 200% to 300% for coordinating 3 to 5 cells, respectively.

However, the implementation of such coordinated multi-point algorithms is considered as rather complex, we demonstrated its feasibility in a first prototyping real-time implementation using the Berlin LTE-Advanced Testbed. Coherent interference nulling was demonstrated over the air while a number of essential network operator requirements have been met. We used distributed synchronization and linked base stations using standard Ethernet. The high latency requirements for the information exchange are met using commercially available network equipment based on the IEEE 802.1q VLAN standard. In our inter-site scenarios, we demonstrated downlink CoMP over 20 MHz bandwidth at 500 m inter-site distance. This is the proof of concept that downlink CoMP can be integrated into the distributed LTE system architecture.

In order to make the promising CoMP technology mature for next generation mobile networks, ongoing studies concentrate on concepts for efficient user grouping, dynamic clustering of base stations [40], [41] as well as concepts to reduce the loss due to impairments caused by delayed channel feedback.

## Acknowledgements

The authors wish to thank F. Bauermeister, K. Börner, H. Droste, A. Forck, G. Kadel, S. Jaeckel, M. Olbrich, T. Wirth and W. Zirwas for their contributions and stimulating discussions. The authors are grateful for a grant from the German Ministry of Education and Research (BMBF) in the project EASY-C under contract No. 01BU0631.

## References

- [1] J. Andrews, W. Choi, and R. Heath, "Overcoming interference in spatial multiplexing MIMO cellular networks," *IEEE Wireless Commun.*, vol.14, no.6, pp.95–104, Dec. 2007.
- [2] L. Zheng and D. Tse, "Diversity and multiplexing: A fundamental tradeoff between in multiple antenna channels," *IEEE Trans. Inf. Theory*, vol.49, no.5, pp.1073–1096, May 2003.
- [3] L. Thiele, M. Schellmann, T. Wirth, and V. Jungnickel, "Interference-aware scheduling in the synchronous cellular multi-antenna downlink," *IEEE 69th Vehicular Technology Conference VTC2009-Spring*, Barcelona, Spain, April 2009.
- [4] P. Baier, M. Meurer, T. Weber, and H. Troger, "Joint transmission (JT), an alternative rationale for the downlink of time division CDMA using multi-element transmit antennas," *Spread Spectrum Techniques and Applications*, 2000 IEEE Sixth International Symposium on, vol.1, pp.1–5 vol.1, 2000.
- [5] S. Shamai and B. Zaidel, "Enhancing the cellular downlink capacity via co-processing at the transmitting end," *Proc. IEEE VTC'01 Spring*, vol.3, pp.1745–1749, 2001.
- [6] T. Weber, I. Maniatis, A. Sklavos, Y. Liu, E. Costa, H. Haas, and E. Schulz, "Joint transmission and detection integrated network (JOINT), a generic proposal for beyond 3G systems," *9th International Conference on Telecommunications (ICT'02)*, vol.3, pp.479–483, Beijing, June 2002.
- [7] A. Goldsmith, S. Jafar, N. Jindal, and S. Vishwanath, "Capacity limits of MIMO channels," *IEEE J. Sel. Areas Commun.*, vol.21, no.5, pp.684–702, June 2003.
- [8] M. Costa, "Writing on dirty paper (corresp.)," *IEEE Trans. Inf. Theory*, vol.29, no.3, pp.439–441, 1983.
- [9] G. Caire and S. Shamai, "On the achievable throughput of a multi-antenna Gaussian broadcast channel," *IEEE Trans. Inf. Theory*, vol.49, no.7, pp.1691–1706, 2003.
- [10] P. Viswanath and D. Tse, "Sum capacity of the vector Gaussian broadcast channel and uplink-downlink duality," *IEEE Trans. Inf. Theory*, vol.49, no.8, pp.1912–1921, 2003.
- [11] H. Huang and S. Venkatesan, "Asymptotic downlink capacity of coordinated cellular networks," *Conference Record of the Thirty-Eighth Asilomar Conference on Signals, Systems and Computers*, 2004., vol.1, pp.850–855, 2004.
- [12] F. Boccardi and H. Huang, "A near-optimum technique using linear precoding for the MIMO broadcast channel," *IEEE International Conference on Acoustics, Speech and Signal Processing, ICASSP 2007*, vol.3, pp.III-17–III-20, April 2007.
- [13] V. Jungnickel, T. Haustein, E. Jorswieck, and C. von Helmolt, "On linear pre-processing in multi-antenna systems," *IEEE Global Telecommunications Conference*, vol.1, pp.1012–1016, Nov. 2002.
- [14] M. Noda, M. Muraguchi, T.G. Khanh, K. Sakaguchi, and K. Araki, "Eigenmode Tomlinson-Harashima precoding for multi-antenna multi-user MIMO broadcast channel," *6th International Conference on Information, Communications Signal Processing*, 2007, pp.1–5, 2007.
- [15] L. Thiele, T. Wirth, K. Börner, M. Olbrich, V. Jungnickel, J. Rumold, and S. Fritze, "Modeling of 3D field patterns of downtilted antennas and their impact on cellular systems," *International ITG Workshop on Smart Antennas (WSA 2009)*, Feb. 2009.
- [16] J. Winters, "Optimum combining in digital mobile radio with cochannel interference," *IEEE J. Sel. Areas Commun.*, vol.2, no.4, pp.528–539, 1984.
- [17] 3GPP TS 36.211 V9.1.0, "E-UTRA — Physical channels and modulation (release 9)," March 2010.
- [18] L. Thiele, M. Schellmann, S. Schiffermüller, and V. Jungnickel, "Multi-cell channel estimation using virtual pilots," *IEEE 67th Vehicular Technology Conference VTC2008-Spring*, May 2008.
- [19] V. Jungnickel, T. Wirth, M. Schellmann, T. Haustein, and W. Zirwas, "Synchronization of cooperative base stations," *IEEE In-*

- ternational Symposium on Wireless Communication Systems 2008 (ISWCS2008), Oct. 2008.
- [20] T. Bonald, "A score-based opportunistic scheduler for fading radio channels," 5th European Wireless Conference, Feb. 2004.
- [21] M. Schellmann, L. Thiele, T. Wirth, T. Haustein, and V. Jungnickel, "Resource management in MIMO-OFDM systems," OFDMA: Fundamentals and Applications, 2009.
- [22] D. Gesbert, S. Kiani, A. Gjendemsj, and G. Ien, "Adaptation, coordination, and distributed resource allocation in interference-limited wireless networks," Proc. IEEE, vol.95, no.12, pp.2393–2409, Dec. 2007.
- [23] 3GPP R1-100928, Alcatel-Lucent, Alcatel-Lucent Shanghai Bell, "Performance with worst companion PMI reporting," 2010.
- [24] D.S. Baum, J. Salo, M. Milojevic, P. Kyösti, and J. Hansen, "MATLAB implementation of the interim channel model for beyond-3G systems (SCME)," May 2005.
- [25] TR 36.814V1.0.0, "Evolved universal terrestrial radio access (E-UTRA); Further advancements for (E-UTRA) physical layer aspects," Feb. 2009.
- [26] V. Jungnickel, M. Schellmann, L. Thiele, T. Wirth, T. Haustein, O. Koch, W. Zirwas, and E. Schulz, "Interference-aware scheduling in the multiuser MIMO-OFDM downlink," IEEE Commun. Mag., vol.47, no.6, pp.56–66, June 2009.
- [27] W. Zirwas, E. Schulz, J.H. Kim, V. Jungnickel, and M. Schubert, "Distributed organization of cooperative antenna systems," European Wireless, Athens, Greece, April 2006.
- [28] V. Jungnickel, L. Thiele, M. Schellmann, T. Wirth, W. Zirwas, T. Haustein, and E. Schulz, "Implementation concepts for distributed cooperative transmission," 42nd Asilomar Conference on Signals, Systems and Computers, Oct. 2008.
- [29] B.L. Ng, J. Evans, S. Hanly, and D. Aktas, "Distributed downlink beamforming with cooperative base stations," IEEE Trans. Inf. Theory, vol.54, no.12, pp.5491–5499, Dec. 2008.
- [30] A. Papadogiannis, E. Hardouin, and D. Gesbert, "Decentralising multi-cell cooperative processing on the downlink: A novel robust framework," EURASIP Journal on Wireless Communications and Networking, Special Issue on Broadband Wireless Access, Aug. 2009.
- [31] W. Zirwas, W. Mennerich, M. Schubert, L. Thiele, V. Jungnickel, and E. Schulz, Cooperative Transmission Schemes, CRC Press, Taylor and Francis Group, 2009.
- [32] L. Thiele, T. Wirth, T. Haustein, V. Jungnickel, E. Schulz, and W. Zirwas, "A unified feedback scheme for distributed interference management in cellular systems: Benefits and challenges for real-time implementation," 17th European Signal Processing Conference (EUSIPCO2009), 2009.
- [33] V. Jungnickel, L. Thiele, T. Wirth, T. Haustein, S. Schiffermüller, A. Forck, S. Wahls, S. Jaekel, S. Schubert, H. Gabler, C. Juchems, F. Luhn, R. Zavrtak, H. Droste, G. Kadel, W. Kreher, J. Mueller, W. Stoermer, and G. Wannemacher, "Coordinated multipoint trials in the downlink," Proc. 5th IEEE Broadband Wireless Access Workshop (BWAWs), co-located with IEEE GLOBECOM 2009, pp.1–7, Honolulu, Hawaii, Nov. 2009.
- [34] V. Jungnickel, A. Forck, S. Jaekel, F. Bauermeister, S. Schiffermüller, S. Schubert, S. Wahls, L. Thiele, T. Haustein, W. Kreher, J. Müller, H. Droste, and G. Kadel, "Field trials using coordinated multi-point transmission in the downlink," Proc. 3rd International Workshop on Wireless Distributed Networks (WDN), Held in Conjunction with IEEE PIMRC 2010, Istanbul, Turkey, Sept. 2010.
- [35] 3GPP TS 36.300V8.2.0, "Technical specification group radio access network; Evolved universal terrestrial radio access (e-utra) and evolved universal terrestrial radio access network (e-utran); Overall description; Stage 2 (release 8)," Sept. 2007.
- [36] M. Trivellato, F. Boccardi, and H. Huang, "Zero-forcing vs. unitary beamforming in multiuser MIMO systems with limited feedback," IEEE 19th International Symposium on Personal, Indoor and Mobile

Radio Communications, PIMRC 2008, pp.1–6, Sept. 2008.

- [37] H. Zhang and H. Dai, "Cochannel interference mitigation and cooperative processing in downlink multicell multiuser MIMO networks," Eurasip Journal on Wireless Communications and Networking, vol.2004, no.2, pp.222–235, 2004.
- [38] H. Huang and D. Samardzija, "Determining backhaul bandwidth requirements of Network MIMO," 17th European Signal Processing Conference (EUSIPCO2009), 2009.
- [39] S. Jaekel, L. Jiang, V. Jungnickel, L. Thiele, C. Jandura, G. Sommerkorn, and C. Schneider, "Correlation properties of large and small-scale parameters from multicell channel measurements," European Conference on Antennas and Propagation (EuCAP 2009), Berlin, Germany, 2009.
- [40] 3GPP R1-093081, "Distributed dynamic CoMP for LTE-Advanced," Aug. 2009.
- [41] L. Thiele, F. Boccardi, C. Botella, T. Svensson, and M. Boldi, "Scheduling-assisted joint processing for CoMP in the framework of the WINNER+ project," Future Network Mobile Summit, Florence, Italy, June 2010.



**Lars Thiele** (lars.thiele@hhi.fraunhofer.de) received the Dipl.-Ing. (M.S.) degree in electrical engineering from the Technische Universität Berlin, Berlin, Germany, in 2005. Currently he is working towards the Dr.-Ing. (Ph.D.) degree with the Fraunhofer Heinrich Hertz Institute (HHI), Berlin. He has contributed to receiver and transmitter optimization under limited feedback, performance analysis for MIMO transmission in cellular OFDM systems and fair-resource allocation. Lars has authored and

co-authored about 40 conference and journal papers in the area of mobile communications.



**Volker Jungnickel** (volker.jungnickel@hhi.fraunhofer.de) received a Dr. rer. nat. (Ph.D.) degree in physics from Humboldt Universität zu Berlin, Germany, in 1995. He worked on semiconductor quantum dots and laser medicine and joined Fraunhofer Heinrich Hertz Institute (HHI) in 1997. Volker is a lecturer at Technische Universität Berlin and head of the cellular radio team at HHI. He has contributed to high-speed indoor wireless infrared links, 1 Gbit/s MIMO-OFDM radio transmission and

initial field trials for LTE and LTEAdvanced. Volker has authored and co-authored about 90 conference and journal papers on communications engineering.



**Thomas Haustein** (thomas.haustein@hhi.fraunhofer.de) received the Dr.-Ing. (Ph.D.) degree in mobile communications from the Technische Universität Berlin, Berlin, Germany, in 2006. In 1997, he was with the Fraunhofer Institute for Telecommunications, Heinrich Hertz Institute (HHI), Berlin, where he worked on wireless infrared systems and radio communications with multiple antennas and orthogonal frequency division multiplexing. He focused on real-time algorithms for baseband processing

and advanced multiuser resource allocation. In 2006, he was with Nokia Siemens Networks, where he conducted research for Long-Term Evolution (LTE) and LTE-advanced. He is currently the Head of the Broadband Mobile Communications Department, HHI.